TRANS-AEGEAN SEISMICITY, SEISMIC HAZARD AND DEFENCES

P. W. BURTON[1] and G-A. TSELENTIS[2]
[1]*University of East Anglia, School of Environmental Sciences, Norwich, UK*
[2]*University of Patras, Seismological Laboratory, Patras, Greece*

Abstract

Observation and analysis of both micro- and macroearthquakes is vital to understanding and preparation of multi-facetted and in-depth earthquake defences. Therefore the paper revisits simple, yet fundamentally important maps of macroearthquake felt effects in Turkey which modern techniques extend to statistically interpretable hazard and zoning maps. Such mapping should ultimately be extended well beyond peak ground acceleration to a larger, more representative suite of earthquake hazard parameters for advisory purposes. Both vigilance and rapid reaction dominate exploitation of microearthquakes. Rapid reaction resulted in a seismic network around the Athens 1999 September 15 earthquake, and 450 locally recorded aftershocks identify the fault plane (strike 117°, dip 52°) consistently with teleseismic observations. Longer term monitoring in central Greece associated with swarms at Pavliani and with Egion 1995 June 15 aftershocks provides physical properties during rupture: stress drop, coseismic slip length etc. and scaling relations between seismic moment and slip. In the case of Pavliani coseismic slip is mapped in 2D throughout a pseudo fault-zone that lacks a history of any major earthquake. The ultimate vigilance and rapid reaction in defence are embodied by earthquake early warning. An embryonic early warning demonstration system associated with liquid natural gas storage near Athens is introduced.

1. Introduction

Analytical use of large and small earthquakes contributes to our understanding of seismicity and ultimately to the means of defending industry and communities against large and damaging events. Small earthquakes can be used for scaling purposes in the modelling of large earthquakes and for characterising swarm seismicity. Defence against large earthquakes can be developed indirectly in terms of hazard and risk zoning and selection of design earthquakes for engineering purposes, and directly through earthquake early warning systems that initiate immediate safety responses when triggered.

N. Görür et al. (eds.),
Integration of Earth Science Research on the Turkish and Greek 1999 Earthquakes, 175–196.
© 2002 *Kluwer Academic Publishers. Printed in the Netherlands.*

Four aspects will be considered briefly:

- Seismic hazard and selection of representative earthquakes in north and west Turkey and the potential for "stacked" hazard criteria.
- Seismogenesis related to microearthquakes and swarms.
- Preliminary results from modelling of the Athens earthquake (1999 September 7, 5.9Mw).
- Development of earthquake early warning systems, an example in Greece.

Seismic hazard has been mapped in Turkey by different means over many years. Work in the 1970s mapped the felt effects of earthquakes throughout Turkey, see Ergünay [8], very effectively (Figure 1). Statistical analysis of the underlying earthquake catalogues has been able to put the earlier "felt effect" maps on a probabilistic basis providing a further foundation for hazard zoning and selection of earthquakes for design purposes [4]. Such methodologies tend to be single-track and produce a free-standing estimate of hazard derived from the one technique. There is the potential to "stack" different hazard criteria (e.g. 100-year expected magnitude, maximum credible earthquake, 100 year expected peak ground acceleration etc.) and form composite hazard maps [30], or even to extend to risk zoning taking into account soil conditions and building stock. Nevertheless, such approaches need steady updating with the advent of new earthquakes and, in the case of Anatolia, the possibility of time variation in the seismicity.

Pure hazard analysis exemplified above tends to overlook the wealth of information provided by careful monitoring of microearthquakes. For example, swarms of microearthquakes observed in central Greece have been analysed in terms of their associated geometry (fault dimension) and kinematics (stress drop during rupture and the amount of coseismic slip). Such analyses allow mapping of cumulative coseismic deformation in an area [5, 15]. One area so mapped appeared slightly anomalous in relation to its rupture properties [15] in the vicinity of what ultimately was the epicentral region of the Egion earthquake in the Corinth Gulf (1995 June 15, 6.2 M_L, [27]). The aftershocks of the Egion earthquake themselves provided further valuable information on scaling properties of earthquakes in Greece [6].

The Athens earthquake of 1999 September 7 occurred eastwards of the known high seismicity in the Corinth Gulf, in an unexpected location: almost a "rogue" earthquake. Once again detailed aftershock monitoring - microearthquakes - has lead to substantial understanding of the main, damaging macroearthquake [28, 29]. The aftershocks during 20 days identify the fault plane as dipping 52 degrees and striking 117 degrees, consistent with teleseismic solutions. The results also indicate two clusters of aftershocks during the first 12 days of observation, consistent with an asperity measuring about 10 km on a fault length of about 10-20 km. The onset of rupture appears to have been abrupt.

The techniques described above enhance our understanding of seismicity at both micro- and macro- level and lead towards earthquake defence with different levels of directness. Ultimately, earthquake defence requires pragmatic action. This can be in the form of decision taking on safe land-use dependant on good seismic zoning maps, aseismically designed buildings constructed on sound earthquake engineering practise, and, growingly, the deployment of earthquake early warning systems to attempt to

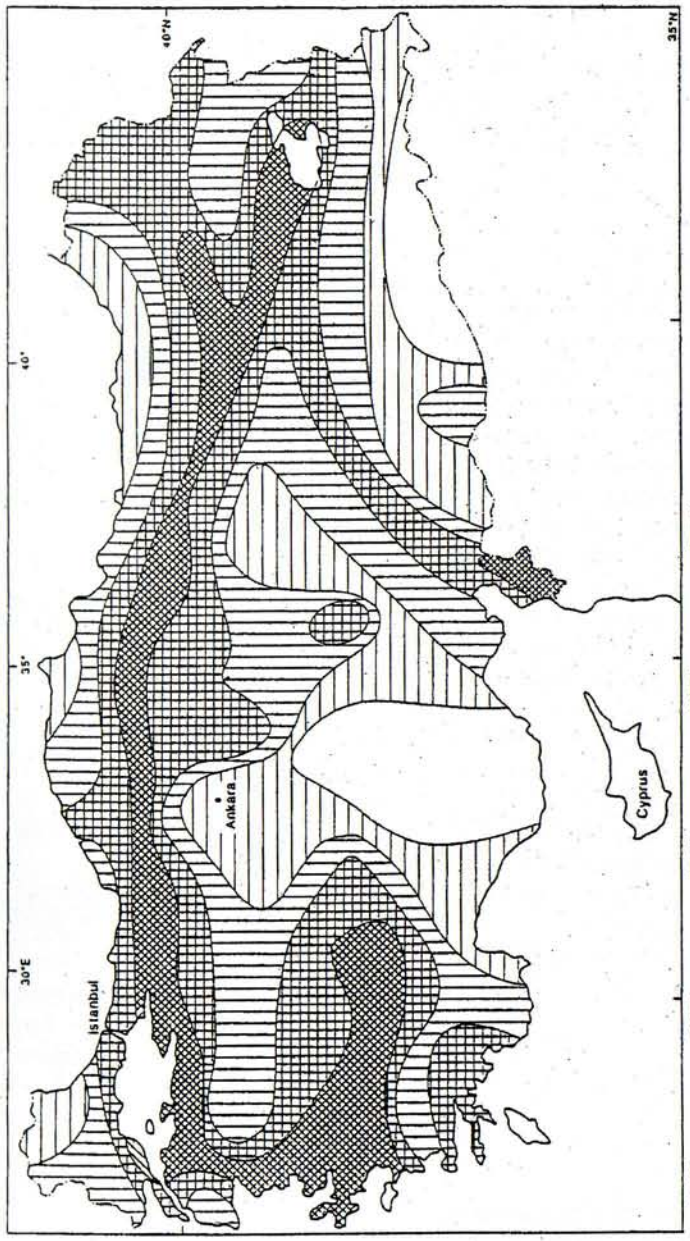

Figure 1. Earthquake zoning map of Turkey arising from the UNDP-UNESCO survey of seismicity in the Balkan region (after Ergunay [8]). There are five zones representative of increasing earthquake impact through zones 1 to 5.

mitigate some of the worst potential effects of earthquake e.g. fire-following earthquake. As example of this is the SHIELD to be deployed in central Greece, focussed around liquid natural gas storage near Athens, by which it is hoped to demonstrate the practicality of early warning at sensitive sites against off-site earthquakes. This early warning system will be co-ordinated by the University of Patras.

2. Seismic Hazard Mapping

Trans-Aegean seismicity spanning Greece and Turkey has been analysed for many years. Indeed, as Papaioannau and Papazachos [19] point out there have been more than 40 scientific publications about seismic hazards in Greece during the last 25 years. Much of this work relates to peak ground acceleration (e.g. see Makropoulos and Burton [14] and much essential review material in Papazachos and Papazachou [20]) but also to macroseismic intensity, because of its direct link to damage. Papaioannau and Papazachos [19] emphasise seismic zonation and intensity and their results complement the New Seismic Code of Greece that divides Greece into four zones of equal seismic hazard (NEAK 1995). The result of this recent analysis is reminiscent of the earlier work for Turkey that produces the five zones of Ergünay's [8] map, here adapted as Figure 1, based entirely on felt effects and intensity analysis. The original red-shaded map corresponding to Figure 1 tells us a great deal of what we need to know about earthquake hazard and risk in Turkey, and it has been available for many years.

Increased quantification of the seismicity phenomena represented by maps like Figure 1, for example, in terms of return periods on earthquakes, appropriate design earthquakes, or earthquakes believed to be maximum in some sense, is an important extension. Three examples for Turkey follow in Figures 2-4; these have been redrawn from the original colour maps provided by Burton *et al.* [4] where the corresponding data and analyses are described in fuller detail than provided here.

The map illustrated in Figure 2 relies principally on extreme value analysis of catalogued earthquake magnitudes. The distribution used here is Gumbel's third asymptotic distribution [10] which has the form

$$P(M) = \left[-\left(\frac{\omega - M}{\omega - u} \right)^{1/\lambda} \right] \qquad (1)$$

in which ω, u and λ are distribution parameters and P(M) is typically the probability that magnitude M (here the surface wave magnitude) is an annual extreme. Adopting extreme value analysis means that the catalogued earthquakes analysed are more likely to be better documented, larger earthquakes of engineering interest. Minor modification to the statistics expressed through equation (1) allows magnitudes corresponding to different return periods to be calculated, as can confidence limits through covariance analysis, or magnitudes with 90% probability of non-exceedance in 50-years etc.

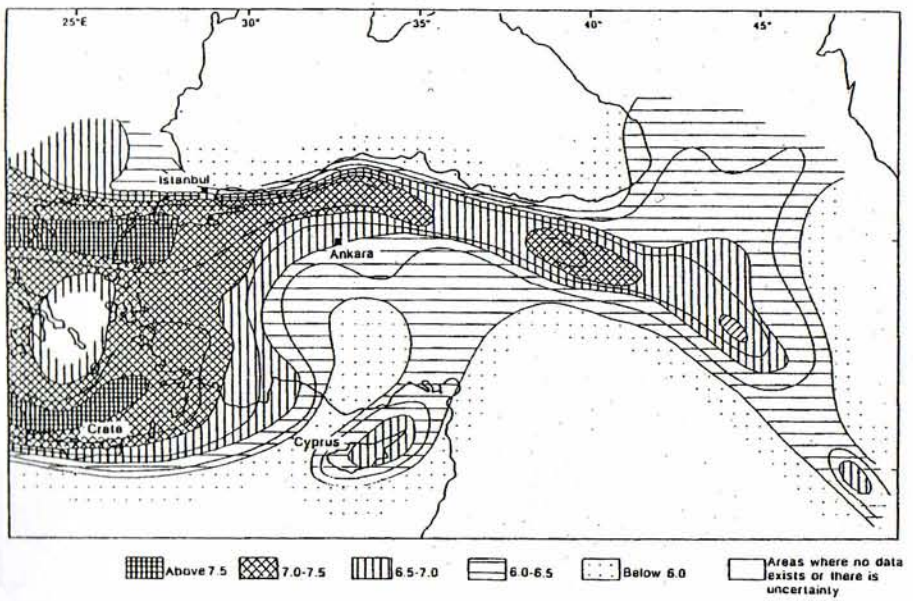

Figure 2. Seventy-five year earthquake magnitudes. The largest earthquake magnitudes expected over a period of seventy-five years predicted using Gumbel's third asymptotic distribution of extreme values (adapted from Burton *et al.* [4]).

In the case of Figure 2, the largest magnitude earthquake expected over a period of seventy-five years, M_{75}, is selected and contoured throughout Turkey. The calculation scheme analyses seismicity in cells of 4° size, overlaps these to provide fuller spatial detail, and attributes the hazard parameter, M_{75}, to the centroid of energy release in the cell. It is this set of centroidal, cellularly overlapping hazard values that is contoured. There are wide regions of western and north-western Turkey that might expect an earthquake in excess of magnitude 7.0 in a seventy-five year period. The question of largest earthquakes is also of interest and this can be investigated by a quite different and non-probabilistic model. The map in Figure 3 illustrates results for maximum credible earthquakes resulting from such a model.

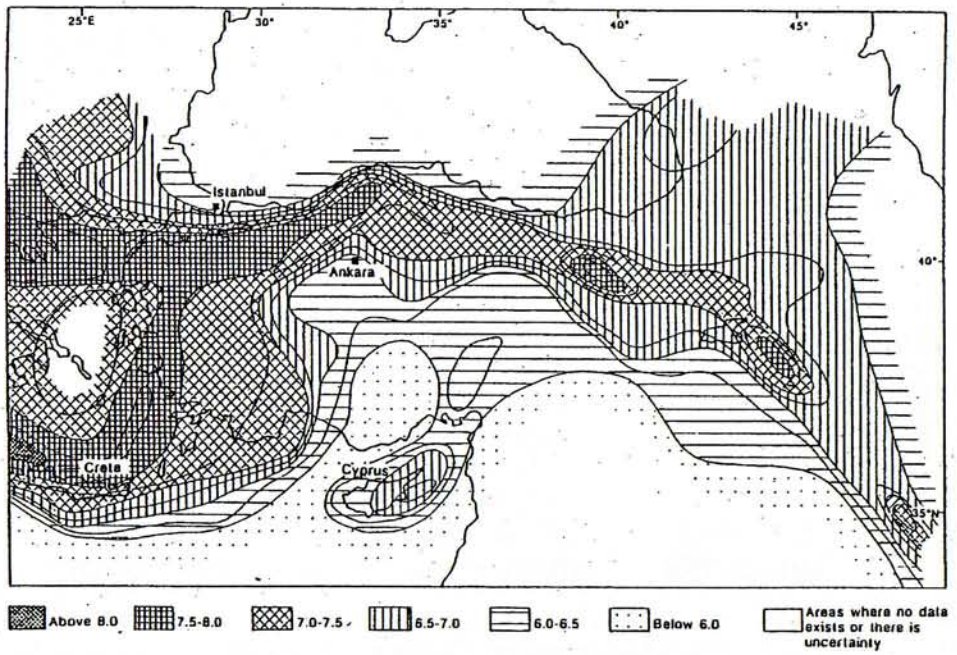

Figure 3. Magnitudes analogous to maximum strain energy: maximum credible earthquakes. Strain energy release determined from cells of seismicity of 4° side is used, and from this the magnitudes analogous to the maximum strain energy conceived possible on this model, are determined throughout Turkey and neighbouring areas (see [4]).

The staccato occurrence of earthquakes lends itself to the staircase model of energy release in Figure 5 of Makropoulos and Burton [13]. This graph of cumulative energy release allows determination of the annual rate of energy release as its simplest result- from the gradient of the central line. However, taking the total energy supply to a region that may be accumulated and released as a constant, means that two outer parallel lines may be drawn to embrace all excursions of the staircase from the mean energy release line. Hence the vertical distance between the two outer enveloping lines estimates the upper limit E_{max} to the accumulating energy that can be released by a single earthquake: E_{max} corresponds to the largest earthquake magnitude M_3 and this is contoured in Figure 3. A corollary to M_3 is the horizontal interval between the enveloping lines that indicates the waiting time, or minimum time, required to accumulate E_{max}, hence an M_3 capability, if no other earthquakes occur in the meantime.

The magnitude of the recent 1999 August 17 Izmit earthquake has generally been adopted as 7.4 M_s from teleseismic and surface rupture data [3, 2] which is entirely consistent with the prior forecast values illustrated in Figure 3.

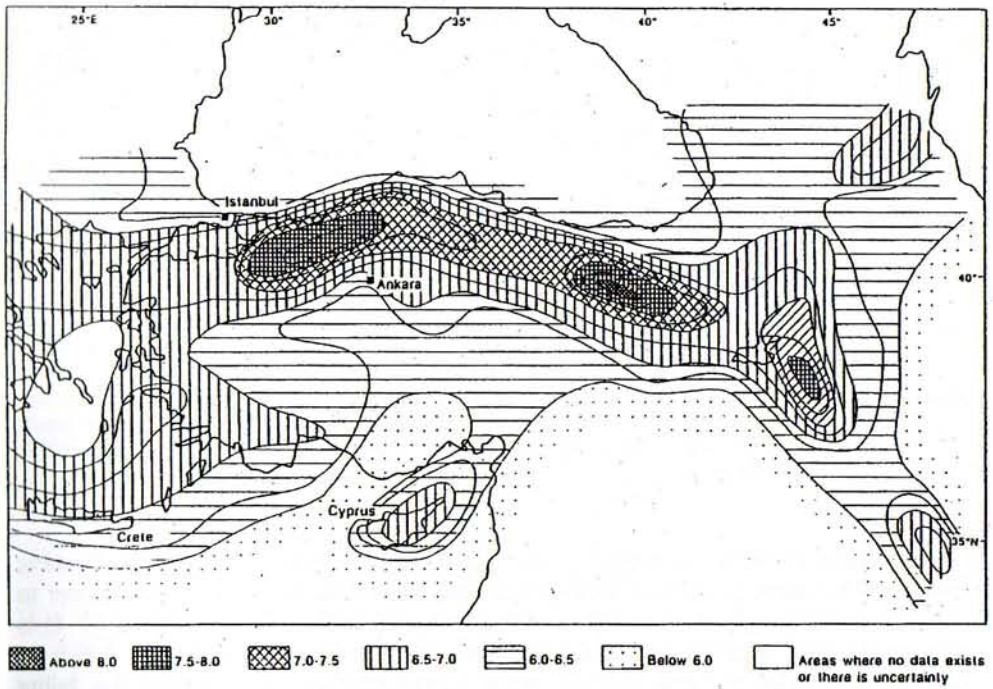

Figure 4. Perceptibility: the magnitudes of locally most perceptible earthquakes. Earthquake magnitude occurrence statistics are combined with regional intensity attenuation laws to indicate the earthquake magnitude which, in principle, is the most likely to be perceived locally at any level of achievable intensity. This is the magnitude locally of the "most perceptible earthquake" (see [4]).

Despite the relatively limited time span of data used to produce this map it appears that the relatively high seismicity rate of the region facilitates consistent estimation of hazard values, with the region of Izmit being close to the contour between 7.0-7.5 and 7.5 upwards largest earthquakes.

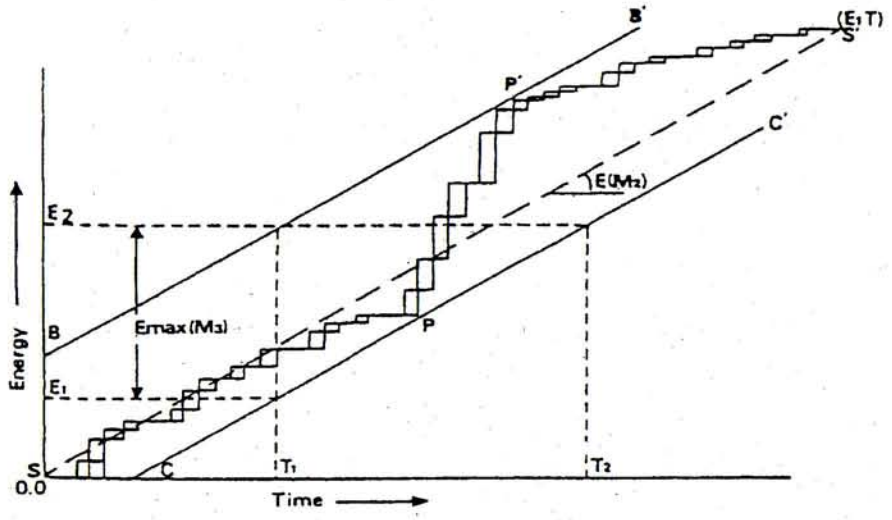

Figure 5. Coseismic strain energy release model. Cumulative earthquake strain energy release with time embraces any evidence of cyclicity in the seismicity history and this model allows simple calculation of an upper limit to strain energy release, Emax (M_3), and hence a maximum credible magnitude, M_3 (see [13]).

A further important, but often elusive, question is how best to select engineering design earthquakes, or scenario earthquakes, for conventional structures. An answer to this question is provided by the map of Figure 4 and methodology of Figure 6. It is obvious that the larger the earthquake then the rarer it occurs; conversely, the larger an earthquake is when it occurs then the greater is the likelihood of feeling it (i.e. being within the "felt" area, or within isoseismal VI corresponding to the likely area of damage, etc.). Referring to Figure 6 it emerges that the product of the probability of an earthquake of size m occurring, $\Phi(m)$, with the probability of experiencing ground motion at least at level x (intensity, PGA etc.), say $P_c(x)$, will have a peak value. Thus the probability of experiencing ground motion level x *associated* with a magnitude m occurrence, $P_p(m|x)$, is

$$P_P(m|x) = \Phi(m)\, P_c(x) \qquad (2)$$

The probabilities $\Phi(m)$ and $P_c(x)$ can be estimated using equation (1) and an appropriate attenuation law respectively. The peaks of P_p are the "most perceptible earthquakes" and although these are not the maximum credible or largest and rarest earthquakes, they will nevertheless be perceptible and cause damage on the greater

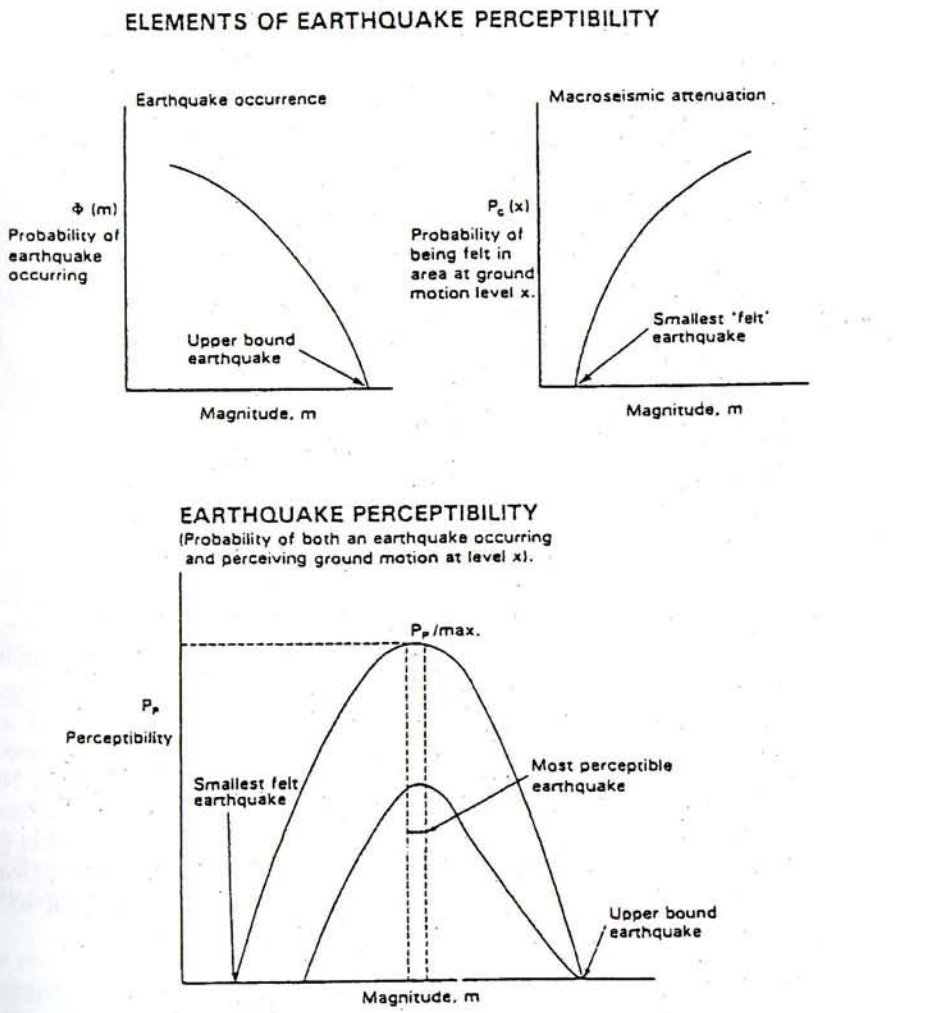

Figure 6. Earthquake "perceptibility" model. The probability of *both* an earthquake occurring *and* it being perceived at ground motion level x (intensity or peak ground acceleration etc.) forms a probability distribution with a peak value. The "most perceptible earthquake" corresponds to this peak probability.

number of occasions. The peaks of P_p are readily associated with a magnitude or energy or seismic moment, and Figure 4 contours the magnitude of the "most perceptible earthquake" throughout Turkey. Despite the general scale of these maps, which are drawn for general guidance rather than exact deduction, it is seen that the Izmit earthquake of magnitude 7.4 M_s is also consistent with the "most perceptible earthquake" analysis for this region.

All of the previous maps have a distinctly individual informative message, and thus a merit. In each case a free-standing estimation of a hazard parameter is derived from a separate technique. There is the possibility to form composite hazard maps resulting from a "stack" of different hazard criteria. The results obtained by Yılmaztürk and Burton [30] from such an approach applied to southern Turkey form Figure 7. In this case four hazard parameters were calculated and individual maps produced. The four hazard parameters used are the 100-year intensity (MSK), magnitude and peak ground acceleration and the maximum credible earthquake. Increasingly onerous combinations of these four parameters are ranked into eight progressive levels in Table 1 corresponding to the properties of the eight zones in the stacked hazard map in Figure 7.

Stacked hazard maps like Figure 7 provide the potential to select earthquake strong motion data, e.g. accelerograms, for design or scenario purposes that correspond to a suite of earthquake hazard criteria (such as Table 1) rather than to just one single and arbitrary criterion (such as a 100-year or 475-year peak ground acceleration in an accelerogram).

There are ways to develop the hazard maps of Figures 1-4 and 7. Their provision of a general image of seismic hazard in Turkey can always be renewed as earthquake catalogues accumulate, extend and improve. There is also the assumption of time-independence in the probabilistic examples that can be refined to take into account earthquake sequencing that is possible along the unusually distinct feature of the North Anatolian fault [1, 26]. However, return periods can be reliably estimated as a Poisson process, even for the Anatolian Fault Zone, as reported by Öncel and Alptekin [16]. There is therefore much useful mapped material available for the consideration ofzoning and design earthquake selection in Turkey that inevitably needs extending to site specific and urban applications by local detailed study.

TABLE 1. A ranking of seismic zones by increasingly onerous combinations of the 100-year intensity I, magnitude M_s, peak ground acceleration PGA, and maximum credible earthquake magnitude M_3

ZONE	I(MSK)	M_s	PGA (cm s^{-2})	M_3
I	≤ 6	≤ 5.0	≤ 60	≤ 6.5
II	5.0-8.5	4.5-6.0	20-80	5.0-6.5
III	6.0-8.5	5.0-6.5	60-100	6.0-6.7
IV	7.0-9.0	5.5-6.5	80-140	6.2-6.7
V	7.9-9.0	6.0-7.0	120-180	6.5-7.2
VI	8.0-8.5	6.5-7.0	160-220	7.0-7.2
VII	8.0-9.2	6.5-7.0	140-340	7.0-7.2
VII	8.5-9.5	6.7-7.6	180-280	7.0-7.5

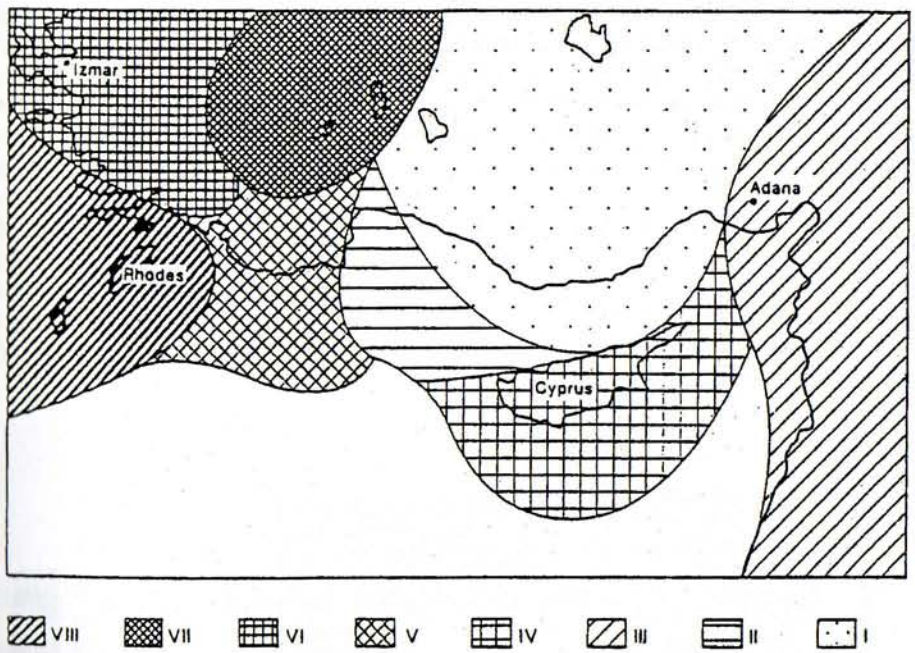

Figure 7. " Stacked" seismic hazard maps: southern Turkey. The map shows seismic zones based on a combination of the distribution of four distinct seismic hazard parameters: 100-year magnitude, intensity (MSK) and peak ground acceleration, and the maximum magnitude M_3 equivalent to the maximum credible strain energy release model (adapted from Yılmaztürk and Burton [30]).

3. Seismogenesis: Micro and Macro Earthquakes, and the Athens Earthquake of 1999 September 7

The previous section emphasized how seismic hazard and seismicity characteristics can be represented by different means for a territory to aid zoning and design earthquake selection - the emphasis was on earthquake magnitude criteria and earthquake impact concepts like perceptibility for Turkey. In contrast, this section will firstly describe the locally detailed information on coseismic crustal deformation that can be obtained from analysis of suites of well-recorded microearthquakes. Secondly, it will consider the complementary nature of teleseismic studies of large earthquakes with local studies of microearthquake aftershocks, and demonstrate a reinforcing consistency between teleseismic and local studies of the Athens 1999 September 7 (5.8 M_b) earthquake. The emphasis now will be Greece.

Microearthquakes recorded near Pavliani in central Greece (Figure 8) were not associated with any large earthquake, nor is there knowledge of any large locally

damaging earthquake historically, they constitute a classic swarm. Spectral analysis of seismograms associated with the microseismicity in Figure 8 allows determination of seismotectonic parameters such as seismic moment, average stress drop, average coseismic slip and source radius etc. as carried out by Burton *et al.* [5] using well established techniques. Correlations obtained between seismic moment M_0 and local magnitude M_L, *and with* average coseismic slip s are good. The resulting equations are

$$\log M_0 = 10.71\ (\pm 0.09) + 0.79\ (\pm 0.04)\ M_L \qquad (3)$$

and

$$\log M_0 = 11.79\ (\pm 0.05) + 1.38\ (\pm 0.07) \log s \qquad (4)$$

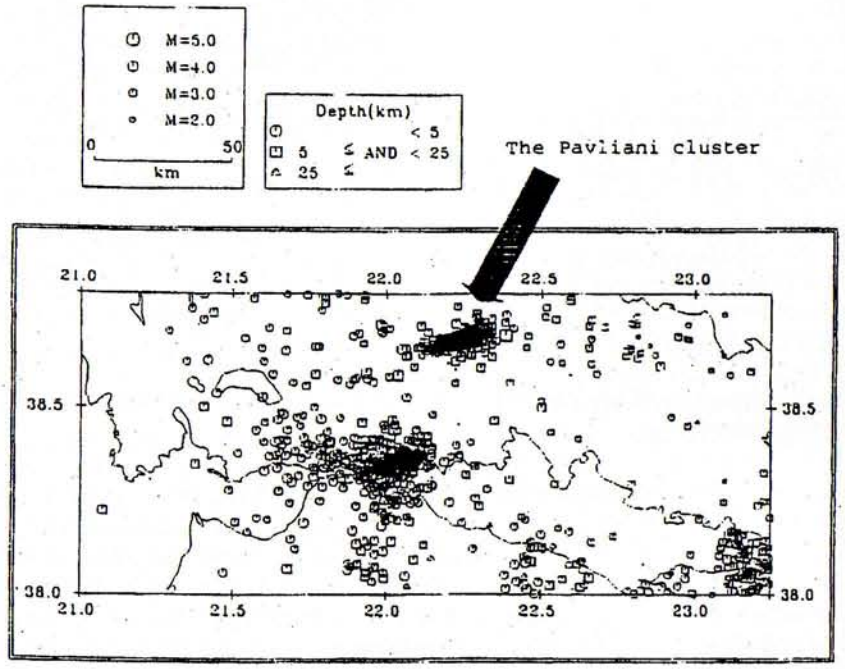

Figure 8. Epicentres of microearthquakes recorded near to Pavliani in central Greece during 1983-84.

and these correlations allow extension of the analysis to the entire suite of microseismicity.

Inspection of the cluster in Figure 8 reveals a narrow epicentral lineation trending WSW to ENE although the foci are distributed through depths deep into the crust, and indicate an approximately vertical pseudo fault-zone. Equations (3) and (4) can be used to calculate the average coseismic slip associated with each earthquake in the swarm, the results mapped onto the vertical pseudo fault-zone, and the average coseismic slips contoured over the fault-zone to produce the distribution illustrated in Figure 9a. Clearly visible is a peak in the individual microearthquake coseismic slips mapped in the shallower eastern part of the fault-zone. This high is created by one of the larger magnitude microearthquakes (local magnitudes analysed in the range 1-4.6 M_L) and this eastern extent of the fault-zone modelled in Figure 9a lies near to a mapped normal fault-the surface projection of this peak is less than 3 km from a normal fault identified by a Mesozoic limestone scarp.

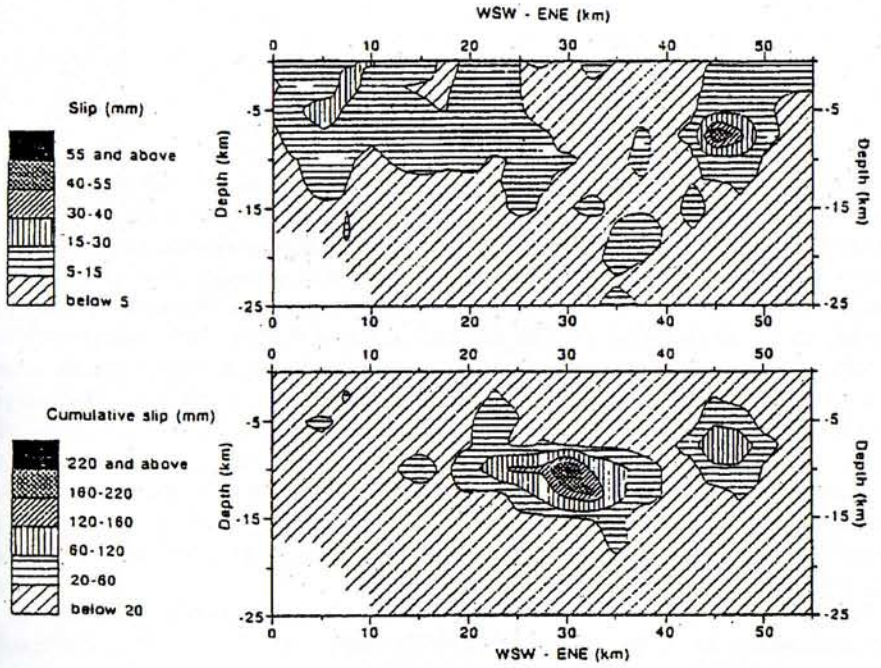

Figure 9. Coseismic crustal deformation from microearthquakes. Cross-section with depth on a fault-zone of contoured values of (a) coseismic slip (upper figure) and (b) cumulative coseismic slip (lower) (also see Figure 8. Figures 8 and 9 after Burton *et al.* [5]).

Coseismic slips can be additive (unlike stress drop) and progressively advance coseismic crustal deformation. Therefore it is possible to add coseismic slips from

individual earthquakes and produce the contoured distribution of cumulative coseismic slip through the fault-zone as illustrated in Figure 9b. A second and larger peak of cumulative coseismic slip now appears in the centre of the fault-zone, the eastern peak is dominated by a small number of larger events and the central peak by a considerably larger number of smaller events. It is interesting to note that the central peak accumulates around 10 km depth, a common seismogenic depth for shallow earthquakes in Greece.

Equations (3) and (4) in which the above analysis of coseismic crustal deformation was founded were obtained in a pure swarm situation, that is one without a strong dominant earthquake. Correlations like equations (3) and (4), but for an aftershock situation, have been obtained recently [6]. These results obtained from the Egion 1995 June 15 (6.5 M_L) earthquake aftershocks are:

$$\log M_o = 9.59\ (\pm 0.22) + 1.19\ (\pm 0.09)\ M_L \qquad (5)$$

and

$$\log M_o = 11.78\ (\pm 0.06) + 1.26\ (\pm 0.09) \log s \qquad (6)$$

The overall differences between equations (3), (4) and (5), (6) are not great, demonstrating that methodology similar to Figure 9 can be reasonably extended to seismogenic fault zones active with large earthquakes and characterised by aftershock sequences rather than swarms. This method could thus be applied to investigate the westward extension of the North Anatolian Fault Zone into the Marmara Sea, south of Istanbul, where the fault path remains an issue. In addition to the above equations, there are also weaker correlations between seismic moment and microearthquake source radius. Microearthquake swarms in the area in the years prior to the Izmit 1999 August 17 earthquake, and then the subsequent aftershocks, analysed in terms of coseismic slip, cumulative coseismic slip, and source radius would be revealing. Cumulative slip would map the path of coseismic crustal deformation through the Marmara Sea, similarly to Figure 9, and mapped (in plan and 3-D) source radii would indicate the extent of connectivity between microearthquake sources and the potential for the path of a major through-going fault.

Tselentis and Zahradnik [28, 29] have used local network observations of microearthquakes to model the Athens 1999 September 7 (5.9 M_w) earthquake. Sargeant *et al.* [24] have modelled the same earthquake using teleseismic observations. Are such disparate methods and observations compatible?

The Seismological Laboratory of Patras University deployed a local network around the epicentral region of the Athens 1999 earthquake and recorded and processed 450 aftershock events [29]. The central cluster of the aftershock distribution, observed in a 2-D depth cross-section that minimized scatter, identified a fault plane striking at 117° with 52° dip. Continuation of this plane to the Earth's surface defines a theoretical fault trace (there was no surface rupture) coincident with the Fili fault, consistent with the studies of Papadopoulos *et al.* [17, 18] and Pavlides *et al.* [21]. Empirical Green's Function (EGF) modelling of the main shock then adopted the fault zone models of

Figure 10. A rectangular fault zone was searched for by Tselentis and Zahradnik [28] that contained the aftershock epicentres when projected onto the Earth's surface and this produced the larger rectangular in Figure 10 of length 20 km along strike and width 16 km along dip. An alternative, strain and stress-swept, source zone without aftershocks was also considered with length 8 km and width 10 km in Figure 10. Rupture propagation nucleating at a matrix of foci was explored [29] using the EGF technique of Irikura and Kamae [11]. The conclusion reached was that the smaller main shock fault zone of 8 x 10 km provides a small rise time and is the most consistent with the three-component broadband station SER that recorded the main shock and aftershock sequence.

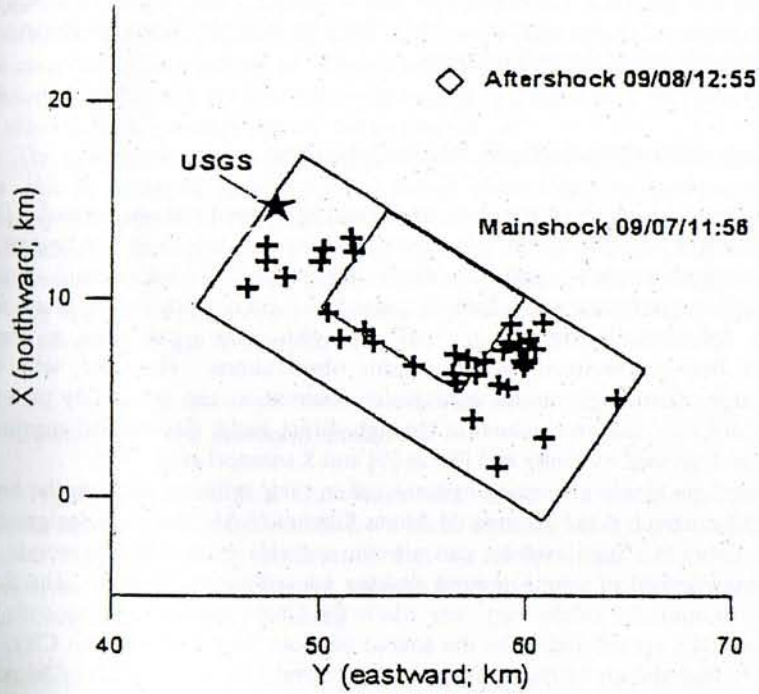

Figure 10. Modelling the Athens 1999 September 15 earthquake: source model derived from regional data and locally recorded aftershocks (after Tselentis and Zahradnik [28]).

Modelling of the broadband teleseismic observations of the Athens 1999 main shock, using 32 three-component broadband stations of the IRIS Global Digital Seismograph Network, has also been carried out by Sargeant *et al.* [24]. Orientation of a double-couple source is found first using the relative amplitudes and polarities of P and the free-surface reflections pP and sP following Pearce [22] and Pearce and Rogers

[23]. Having fixed the orientation of the double couple modelling of the seismograms then continues using finite 2-D dislocations [25] as simple earthquake sources following Douglas *et al.* [7]. First results adopted a circular source model but it was found that an elliptical rupture with an accompanying simpler, and geologically more realistic seismic velocity structure, also allowed modelling of source directivity evident in the teleseismic observations. Whether this directivity is a vital factor contributing to the regional pattern of strong motion observed locally in Greece remains to be assessed fully. The preferred model of Sargeant *et al.* [24] adopts an elliptical rupture that has major axis 8.0 km and minor axis 7.5 km at a depth of 10 ($\pm$ 2) km, the stress drop is 11 bars and associated seismic moment 9.033 (+0.655/-2.445) x 10^{17} Nm. The fault plane solution in terms of strike, dip and rake is 115°, 60°, -80° respectively, broadly consistent with other published studies. The dimensions of the rectangular source zone with eccentric focus finally preferred by Tselentis and Zahradnik [28, 29] is 8 x 10 km, in strong agreement with the dimensions of the 8 (major axis) x 7.5 (minor) km elliptical source preferred by Sargeant *et al.* [24]. Both have implications for directivity observable in the teleseismic and regional data.

4. Development of Earthquake Early Warning Systems

The previous sections have concentrated on traditional aspects of seismic hazard. This included hazard maps for Turkey to aid zoning, earthquake selection for design or scenario and similar purposes, and the direct observation of micro and macro earthquakes in seismogenic zones to establish individual source rupture parameters and general crustal deformation patterns in fault zones-this also established a useful complementarity between regional and teleseismic observations. However, with the advent of real-time seismology careful earthquake observation can growingly provide practical urban defence and loss reduction through direct early warning of imminent strong shaking as described by Goltz and Flores [9] and Kanamori *et al.* [12].

Although earthquake early warning systems are in their infancy, perhaps the best-known successful example is the Sistema de Alerta Sismica (SAS) that was designed to protect Mexico City [9]. Such systems can provide seconds, even 10s of seconds, of warning before the arrival of strong ground shaking caused by earthquake. The SAS was designed to monitor the subduction zone where the Cocos plate moves beneath the North American plate, considered to be the source of most danger to Mexico City. A magnitude 7.2 earthquake on 1995 September 14 occurred 190 miles south of Mexico City and 72 s prior warning was received. Although only minor damage occurred the potential for urban protection was clear.

Lesser amounts of warning can be exploited if the early warning system can be harnessed to a clear purpose. The example we give here is the SHIELD, which is being developed for deployment in central Greece by a consortium including Patras University and the University of East Anglia, and is focussed on the liquid natural gas storage near to Athens. It is intended to develop this system to demonstrate the practicality of early warning to help protect selected and sensitive sites in Greece against off-site strong earthquakes.

The consequences of the outbreak of local fires as a secondary hazard are well known and in the worst cases the remote potential for conflagration is horrific. For example, in the catastrophic Kwanto, Japan earthquake of 1923 September 1, over 100,000 people lost their lives, of these about 68,000 died in widespread fires in Tokyo. Although building styles are now different, the secondary earthquake hazard of fire fuelled by gas supply is potentially horrific. Although it is right that well engineered structures should be the first line of aseismic defence through the implementation of appropriate regulations and codes, early warning also holds the key to further safety measures. There are major natural gas supply pipelines and storage facilities in Greece (Figure 11) including a major depot for liquid natural gas storage at Revithoussa, west of Athens, which is sketched in Figure 12. The first focus of the demonstration SHIELD will be for the alert window to provide opportunity for automatic safe shutdown procedures to mitigate secondary hazards associated with hydrocarbon release at the Revithoussa site. Secondly, the SHIELD will focus on the provision of the opportunity for automatic safety-first shutdown of gas supplies at the point of delivery to a community in a suburb of Athens, with the capability of provision of a warning of imminent earthquake so that simple measures (extinguishing of flames and switching off electrical and gas appliances) can be carried out.

The general principles of the scheme are illustrated in Figure 13. Individual sensor sets will be assigned to monitor for strong ground shaking associated with specific seismogenic sources or zones, and the whole array of sensor sets will relay information to a Central Command and Control Processor. This Central Command and Control Processor will assess the SHIELD data and assess when early warning conditions might prevail, and provide the opportunity for early warning at the Revithoussa storage site and at the point of gas delivery in an Athens suburb.

5. Conclusions and Recommendations

Four types of seismological knowledge and research methods that can contribute to defence against large earthquakes have been discussed and these ranged from seismic hazard mapping, through observation and use of local and teleseismic monitoring to investigate individual earthquake rupture properties and crustal deformation, to real-time seismology and early warning.

- Seismic hazard has been investigated and mapped in Greece and Turkey for many years. Existing hazard maps usually provide reliable general guidance, "rogue" earthquakes like Athens 1999 September 7 notwithstanding. The following are considered to be useful steps.
  - Earthquake catalogues, particularly for Turkey, should be upgraded where necessary and made generally available for ease of access through a central scientific web site.
  - It would be beneficial if existing seismic hazard maps were reassessed using updated catalogues, and,

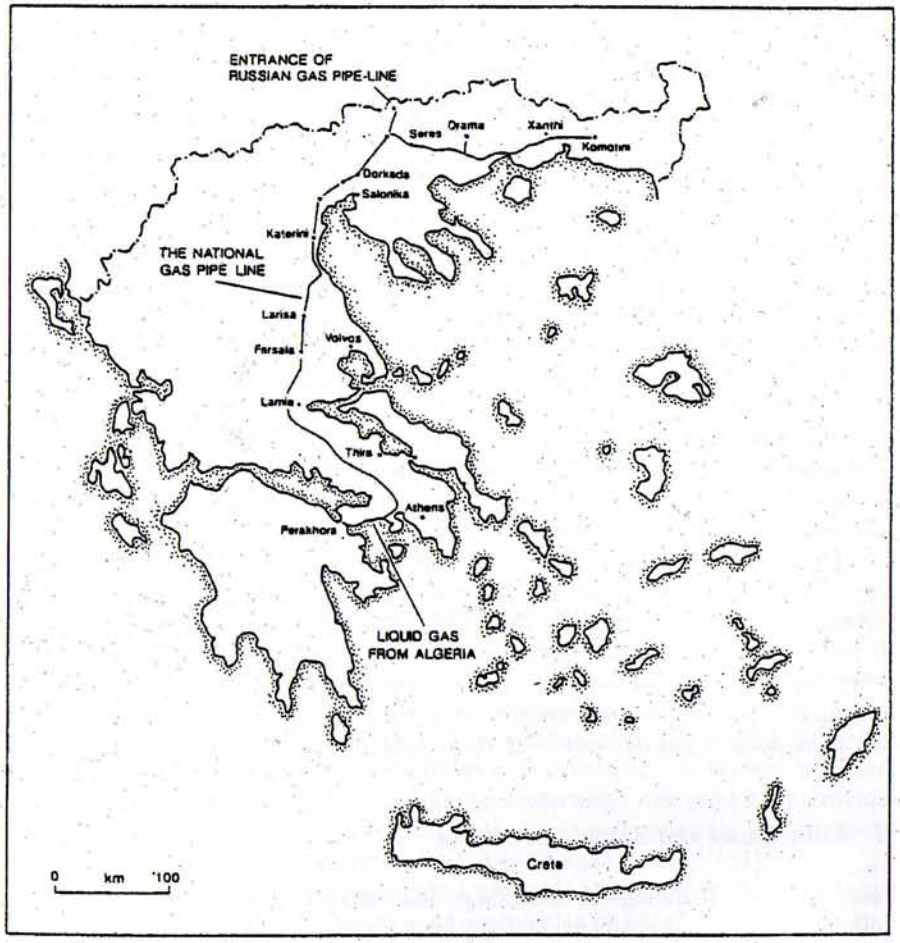

Figure 11. Earthquake early warning: a Demonstration Project in Greece. Oil and natural gas import routes to Greece

- seismic hazard analysis and mapping should attempt to extend beyond PGA mapping to embrace different hazard parameters (e.g. "most perceptible earthquake" and suites of alternative seismic hazard characteristics that can be synthesised into "stacked" seismic hazard maps) to facilitate selection of engineering design and scenario earthquakes.

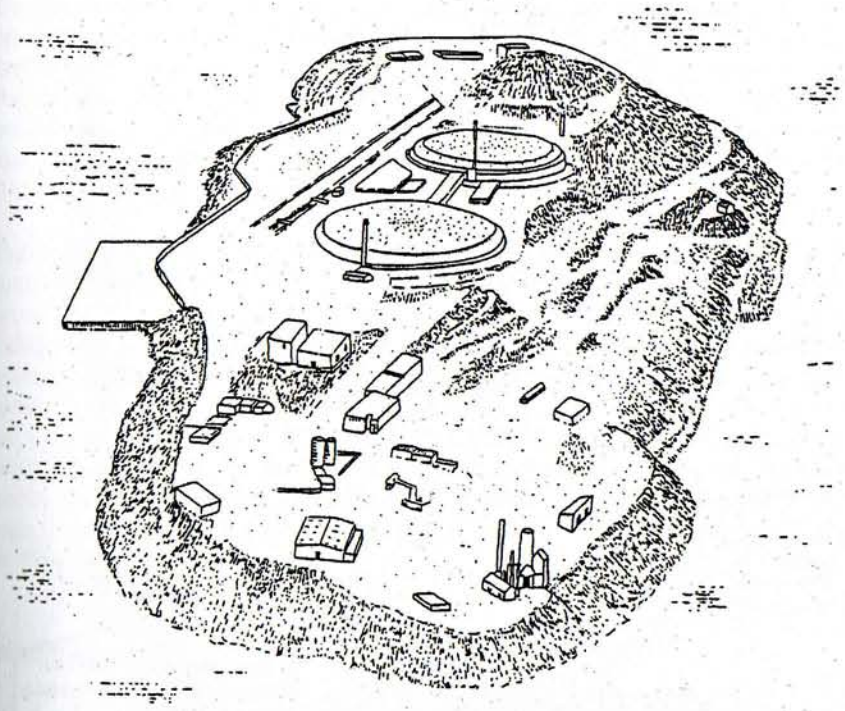

Figure 12. Earthquake early warning: a Demonstration Project in Greece. The caps of two liquid natural gas storage vessels at Revithoussa near Athens.

- Careful monitoring (and associated investment in networks) of microearthquakes by local networks and macroearthquakes by both teleseismic and local networks is vital. Microearthquake data has provided results on seismotectonic rupture properties in central Greece allowing scaling relations to be reliably determined between seismic moment and magnitude and properties such as average coseismic slip in both swarm (Pavliani) and aftershock (Egion 1995 June 15) situations. These results in turn have allowed a valuable extension to conventional methods, facilitating mapping of coseismic crustal deformation in fault-zones. Secondly, both teleseismic and local aftershock observations have reliably and consistently produced seismotectonic results, linking the Athens 1999 earthquake with the surface feature of the Fili fault. Both sets of observations consistently determined a source rupture model of around 8 x 10 km rectangle or 8 x 7.5 km ellipse, with eccentric focus, accommodating source directivity as inferred from both local and teleseismic data. Some of these microearthquake techniques could be applied practically and beneficially.

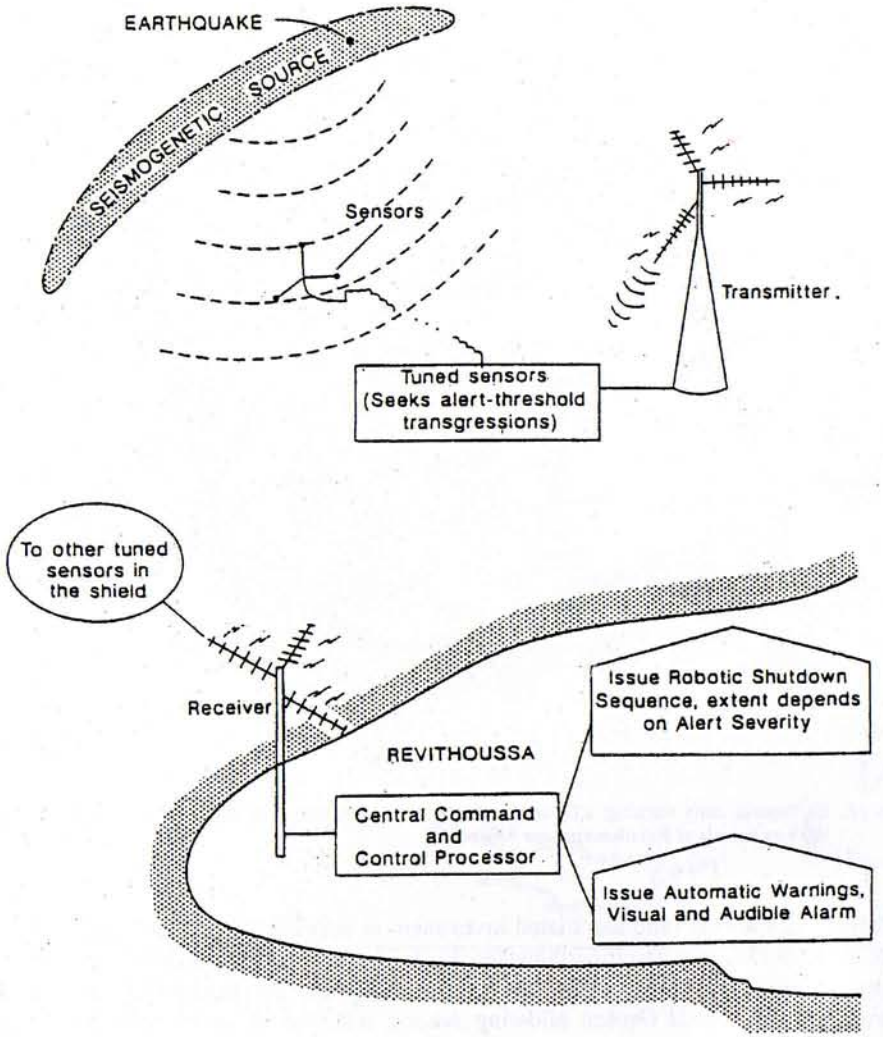

Figure 13. Earthquake early warning: a demonstration project in Greece. Schematic of early warning network principles for Greece.

- The westward extension of the Anatolian Fault Zone into the Marmara Sea remains an issue. Microearthquake swarms prior to, and aftershocks occurring since, the Izmit 1999 earthquake should be analysed to assess cumulative coseismic slips (hence coseismic crustal deformation). Measurement, and 3-D mapping, of the seismotectonic source dimensions (from radii) of these microearthquakes would indicate the extent of connectivity between these micro sources and help to illuminate the path of any through-going fault in the Marmara Sea.

- Earthquake early warning devices and techniques should be developed in Greece and Turkey. Such devices can not be expected to provide the relatively long alert windows associated with the SAS warnings to Mexico City arising from Cocos subduction earthquakes. They should be focussed on selected installations and potentially hazardous situations to complement earthquake engineering based on sound codes and regulations. The SHIELDS early warning system is being designed as a Demonstration Project in Greece to highlight the potential to provide an early warning capability, to mitigate against the secondary hazard of fire-following earthquake, when such a situation could be made much worse by the presence of natural gas. The SHIELDS Demonstration Project will be reported on elsewhere as it develops.

Acknowledgements

Parts of this work have or are being supported by EC Inco-Copernicus Project IC15-CT96-0204, by NATO CRG 940718 and by EC Directorate-General for Energy NNE5/1999/381.

References

1. Ambraseys, N.N. (1970) Some characteristic features of the Anatolian fault zone, *Tectonophysics,* **9**, 143-165.
2. Ambraseys, N.N. and Jackson, J.A. (2000) Seismicity of the Sea of Marmara (Turkey) since 1500, *Geophys. J. Int,* **141**, F1-F6.
3. Barka, A. (1999) The 17 August 1999 Izmit earthquake, *Science,* **285**, 1858-1859.
4. Burton, P.W., McGonigle, R.W., Makropoulos, K.C. and Ucer, S.B. (1984) Seismic risk in Turkey, the Aegean, and the eastern Mediterranean: the occurrence of large magnitude earthquakes, *Geophys. J. R. Astr. Soc.,* **78**, 475-506.
5. Burton, P.W., Melis, N.S. and Brooks, M. (1995) Coseismic crustal deformation on a fault zone defined by microseismicity in the Pavliani area, central Greece, *Geophys. J. Int,* **123,** 16-40.
6. Burton, P.W. and Xu, Y. (1999) The Egion earthquake of 1995 June 15: Results for rupture properties of the aftershocks, *Inco-Copernicus Project Reference Number IC15-CT96-0204,* also see http://karel.troja.mff.cuni.ca/Greece/
7. Douglas, A., Young, J.B. and Hudson, J.A. (1974) Complex P-wave seismograms from simple earthquake sources, *Geophys. J.R. Astr. Soc.,* **37**, 141-150.
8. Ergünay, O. (1974) Earthquake zoning map of Turkey, *UNDP-UNESCO survey of seismicity of Balkan region, Symp. Seismic Zoning Map*, May, Bucharest.
9. Goltz, J.D. and Flores, P.J. (1997) Real-time earthquake early warning and public policy: a report on MexicoCity's Sistema de Alerta Sismica, *Seism. Res. Lett.,* **68**, 727-733.

10. Gumbel, E.J. (1958) *Statistics of Extremes*, Columbia University Press, New York.
11. Irikura, K. and Kamae, K. (1994) Estimation of strong motion in broad-frequency band based on a seismic source scaling model and an empirical Green's function technique, *Ann. di Geofisica,* **37**, 1721-1743.
12. Kanamori, H., Hauksson, E. and Heaton, T. (1997) Real-time seismology and earthquake hazard mitigation, Nature **390**, 461-464
13. Makropoulos, K.C. and Burton, P.W. (1983) Seismic risk of circum-Pacific earthquakes. I: Strain energy release, *Pure Appl. Geophys.,* **121**, 247-267.
14. Makropoulos, K.C. and Burton, P.W. (1985) Seismic hazard in Greece. II: Ground acceleration, *Tectonophysics,* **117**, 259-294.
15. Melis, N.S., Burton, P.W. and Brooks, M. (1995) Coseismic crustal deformation from microseismicity in the Patras area, western Greece, *Geophys. J. Int.,* **122,** 815-836.
16. Oncel, A.O. and Alptekin, O. (1999) Effect of aftershocks on earthquake hazard estimation: an example from the North Anatolian Fault Zone, *Natural Hazards,* **19**, 1-11.
17. Papadopoulos, G.A., Baskoutas, I., Chouliaras, G., Drakotos, G., Kalogeras, I., Karastathis, M., Latoussakis, I., Makaris, D., Melis, N., Panapoulou, G., Papanastassiou, D., Pappis, I., Tassos, S., Plessa, A. and Stavrakakis, G. (1999) Seismological aspects of the Athens earthquake of 7 September 1999, *Preliminary Results, Advances on Natural Hazards Mitigation: Experiences from Europe and Japan*, 73-79.
18. Papadopoulos, G.A., Drakatos, G., Papanastassiou, D., Kalogeras, I. and Stavrakakis, G. (2000 Preliminary results about the catastrophic earthquake of 7 September 1999 in Athens, Greece, *Seism. Res. Lett.,* **71**, 318-329.
19. Papaioannou, Ch. A. and Papazachos, B.C. (2000) Time-independent and time-dependent seismic hazard in Greece based on seismogenic sources, *Bull. Seism. Soc. Am.,* **90**, 22-33.
20. Papazachos, B.C. and Papazachou, C.B. (1997) *The Earthquakes of Greece*, P. Ziti and Co., Thessaloniki.
21. Pavlides, S.B., Papadopoulos, G.A. and Ganas, A. (1999) The 7 September 1999 unexpected earthquake of Athens: Preliminary results on the seismotectonic environment, *Advances on Natural Hazards Mitigation: Experiences from Europe and Japan*, p. 80-85.
22. Pearce, R.G. (1977) Fault plane solutions using relative amplitudes of P and pP, *Geophys. J.R. Astr. Soc.*, **50**, 381-394.
23. Pearce, R.G. and Rogers, R.M. (1989) Determination of earthquake moment tensors from teleseismic relative amplitude observations, *J. Geophys. Res.,* **B1**, 775-786.
24. Sargeant, S.L., Burton, P.W., Douglas, A. and Evans, J.R. (2000 Telseismic waveform modelling of the Athens earthquake, September 7, 1999, *Natural Hazards* (submitted).
25. Savage, J.C. (1966) Radiation from a realistic model faulting, *Bull. Seism. Soc. Am.,* **56**, 577-592.
26. Stein, S.R., Barka, A. and Dietrich, H.J. (1997) Progressive failure on the North Anatolian fault since 1939 by earthquake stress triggering, *Geophys. J. Int.,* **128**, 594-604.
27. Tselentis, G-.A., Melis, N., Sokos, E. and Papatsimpa, K. (1996) The Egion June 15, 1995 (6.2 ML) earthquake, Western Greece, *Pure Appl. Geophys.,* **147,** 83-98.
28. Tselentis, G-A. and Zahradnik, J. (2000) Aftershock monitoring of the Athens earthquake of 7 September 1999, *Seism. Res. Lett.,* **71**, 330-337.
29. Tselentis, G-.A. and Zahradnik, J. (2000) The Athens earthquake of September 7, 1999, *Bull. Seism. Soc. Am.* [submitted].
30. Yılmaztürk, A. and Burton, P.W. (1999) An evaluation of seismic hazard parameters in southern Turkey, *J. Seismology,* **3,** 61-81.